

Research Article

Synthesis and Experimental Validation of New Designed Heterocyclic Compounds with Antiproliferative Activity versus Breast Cancer Cell Lines MCF-7 and MDA-MB-231

Vincenza Barresi,¹ Carmela Bonaccorso,² Domenico A. Cristaldi,² Maria N. Modica,³ Nicolò Musso,¹ Valeria Pittalà,³ Loredana Salerno,³ and Cosimo G. Fortuna²

¹Department of Biomedical and Biotechnological Sciences, University of Catania, Viale A. Doria 6, 95125 Catania, Italy

²Department of Chemical Sciences, University of Catania, Viale A. Doria 6, 95125 Catania, Italy

³Department of Drug Sciences, University of Catania, Viale A. Doria 6, 95125 Catania, Italy

Correspondence should be addressed to Valeria Pittalà; vpittala@unict.it

Received 10 November 2016; Revised 13 February 2017; Accepted 26 February 2017; Published 2 April 2017

Academic Editor: Oliver Sutcliffe

Copyright © 2017 Vincenza Barresi et al. This is an open access article distributed under the Creative Commons Attribution License, which permits unrestricted use, distribution, and reproduction in any medium, provided the original work is properly cited.

Recent drug discovery efforts are highly focused towards identification, design, and synthesis of small molecules as anticancer agents. With this aim, we recently designed and synthesized novel compounds with high efficacy and specificity for the treatment of breast tumors. Based on the obtained results, we constructed a Volsurf+ (VS+) model using a dataset of 59 compounds able to predict the *in vitro* antitumor activity against MCF-7 cancer cell line for new derivatives. In the present paper, in order to further verify the robustness of this model, we report the results of the projection of more than 150 known molecules and 9 newly synthesized compounds. We predict their activity versus MCF-7 cell line and experimentally verify the *in silico* results for some promising chosen molecules in two human breast cell lines, MCF-7 and MDA-MB-231.

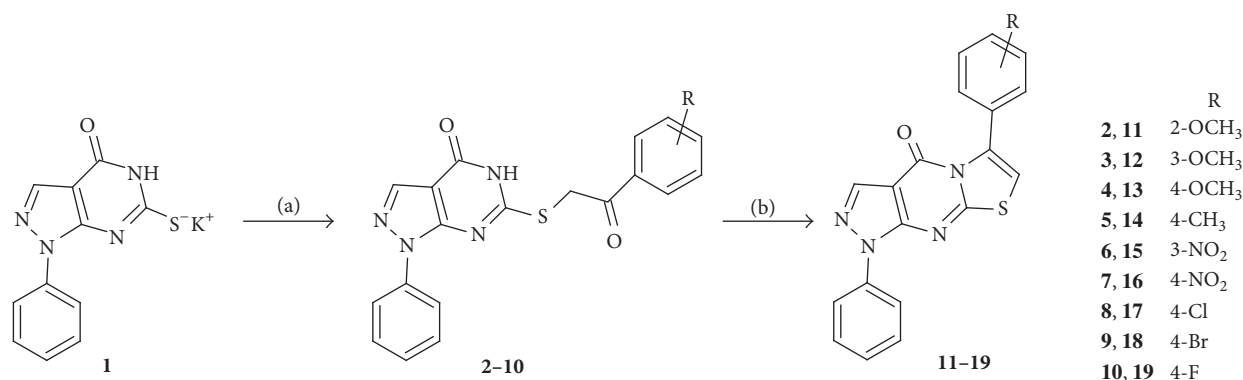
1. Introduction

Despite continued research efforts, cancer remains one of the biggest threats to human health. In the United States, it is the second highest cause of death and is likely to soon replace heart disease as the leading cause [1]. Breast cancer is the most common cancer in women worldwide, with nearly 1.7 million newly diagnosed cases in 2012 (second most common tumor overall) [2, 3]. This represents about 12% of all new cancer cases and 25% of all cancers in women. A number of risk factors have been identified, such as a strong family history of breast cancer, weight gain, smoke, menopausal hormone therapy (MHT), and alcohol consumption [4–6]. However, the causes of the disease are not yet fully understood. Treatment generally involves surgery, radiation, chemotherapy, hormone therapy, and/or targeted therapy. New anticancer agents with unique mechanisms of action have been developed; however, many of them have not been therapeutically useful due to low tumor selectivity or to side

effects. As an example, the US Food and Drug Administration (FDA) recently retired bevacizumab, approved for the treatment of metastatic breast cancer, because of potentially adverse side effects and minimal therapeutic benefit [7].

Drug discovery efforts are highly focused towards design and synthesis of small molecules as anticancer agents [8]. In parallel, most efforts are devoted towards the “drug-repositioning process” as an alternative drug development strategy [9]. This approach gives an opportunity to find new uses of existing drugs or molecules with a tremendous savings of time and money.

During the years, a wide range of small molecules based on heterocyclic ring systems have been studied for the development of novel lead compounds in the drug discovery paradigm. A number of the heterocyclic nuclei can be regarded as “privileged scaffolds” [10] because they are ubiquitous in drug molecules. Since they possess hydrogen bond donors and acceptors in a rigid framework, they can therefore effectively interact with target enzymes and



SCHEME 1: Reagents and conditions: (a) $\text{ClCH}_2\text{COC}_6\text{H}_4\text{R}$, EtOH, reflux; (b) PPA, room temperature or H_2SO_4 conc., 140°C .

receptors *via* hydrogen bond interactions. They can enhance binding affinity and improve *in vitro* potency. Heterocycles can modulate lipophilicity of the drug molecules or improve aqueous solubility of the compounds, thus providing desired pharmacokinetic and pharmaceutical properties [11].

These premises prompted us to design and synthesize novel compounds with high efficacy and specificity for the treatment of breast tumors. In 2013, this research group reported the design and synthesis of new heterocyclic compounds [12]. To fasten the lead discovery process, a Volsurf+ (VS+) model was constructed using a dataset of 59 compounds able to predict the *in vitro* antitumor activity against MCF-7 cancer cell line for the new derivatives. The use of Volsurf+ for *in silico* models generation is a well established procedure, with proved efficacy [13, 14]. Novel compounds when tested *in vitro* showed a significant agreement with *in silico* predictions. In the present paper, in order to verify further the robustness of this model and to apply the drug-repositioning concept, we report the results of the projection of 176 derivatives. Among them, 167 were previously synthesized for other applications such as α_1 adrenergic, 5-HT_{1A} serotonergic, or endothelin receptor ligands and antiproliferative compounds active in prostate tumor cell lines [15–25]. Moreover, 9 compounds were designed and synthesized based on the recent literature [26–28] reporting the activity of pyrimidinketones against MCF-7 cell line. The new compounds retain the same heterocyclic core with respect to the literature ones, modified by fusion with thiophene and pyrazole rings with different substituents. Such modifications should improve the antiproliferative activity reported in literature for similar compounds. All the 176 structure formulas were reported in Supporting Information (SI) (in Supplementary Material available online at <https://doi.org/10.1155/2017/9729284>). The generated dataset is made up of 7 subsets based on different chemical scaffolds, namely, pyrrolopyrimidindione, pyrimidinketone, benzyloxyindole, indole, long chain arylpiperazines (LCAPs), quinoline, and thiophene derivatives (SI). These subsets share the common characteristic of being composed of small molecules possessing a heterocyclic core. The cores were chosen based on the idea of using privileged scaffolds [10]. The term “privileged scaffolds” was first coined

by Evans et al. in the late 1980s [29], referring to scaffolds seemingly capable of serving as ligands for a diverse array of receptors, for example, indole, quinoline, and arylpiperazines.

All these 176 structures represented our training set that is very different compared to the 59 compounds of the test set because of the lack of the ethylenic bond that is the main feature of the test set.

Herein, we predict the subsets activity versus MCF-7 cell line and experimentally verify the *in silico* results for promising chosen molecules in two human breast cell lines, MCF-7 and MDA-MB-231.

2. Material and Methods

2.1. Chemistry. The synthetic procedure for the preparation of new compounds 2–19 is reported in Scheme 1. The monopotassium salt of 1,5,6,7-tetrahydro-1-phenyl-6-thioxo-4*H*-pyrazolo[3,4-*d*]pyrimidin-4-one (1) [30] reacted with substituted phenacyl chloride at reflux in ethanol to give the corresponding 1,5-dihydro-6-[(2-substitutedphenyl)-2-oxoethylthio]-1-phenyl-4*H*-pyrazolo[3,4-*d*]pyrimidin-4-ones (2–10). Compounds 2–4, 6, and 7 were cyclized to the corresponding 6-(2-substitutedphenyl)-1-phenyl-pyrazolo[3,4-*d*]thiazolo[3,2-*a*]pyrimidin-4(1*H*)-ones (11–13, 15, and 16) by heating in presence of an excess of polyphosphoric acid. Compounds 14 and 17–19 were obtained by cyclization of derivatives 5 and 8–10 at room temperature using concentrated sulfuric acid.

2.1.1. Synthetic Procedures. Melting points were obtained by a Gallekamp apparatus provided with a digital thermometer MFB-595 using glass capillary tubes and are uncorrected. Elemental analyses for C, H, N, and S were carried out with a Carlo Erba Elemental Analyzer Mod. 1108 instrument and were within $\pm 0.4\%$ of theoretical values. IR spectra were obtained in KBr disks using a Perkin Elmer 1600 Series FT-IR spectrometer. ¹H NMR spectra were performed at 200 MHz with a Varian Inova Unity 200 spectrometer in DMSO-*d*₆ as solvent. Chemical shifts are reported in δ values (ppm) and coupling constants (*J*) are given in hertz

(Hz); tetramethylsilane was used as internal standard. The purity of all synthesized compounds was checked on thin-layer chromatography, using Merck aluminum sheet coated with silica gel 60 F₂₅₄ and visualization by UV light at 254 and 366 nm of wavelength. All chemicals and solvents were purchased from commercial vendors and were used without further purification.

2.1.2. General Procedure for the Synthesis of 1,5-Dihydro-6-[(2-substitutedphenyl)-2-oxoethyl]thio]-1-phenyl-4H-pyrazolo[3,4-d]pyrimidin-4-one (2-10). A mixture of monopotassium salt **1** (3.55 mmol) and of the appropriate phenacyl chloride (3.55 mmol) was refluxed under stirring in ethanol (30 mL) for 3 h. After cooling, the precipitate was collected, washed with ethanol, dried, and recrystallized from a mixture of ethanol/dioxane with the exception of compound **8** (recrystallization solvent: ethanol). Using this procedure the following compounds were obtained.

2.1.3. 1,5-Dihydro-6-[[2-(2-methoxyphenyl)-2-oxoethyl]thio]-1-phenyl-4H-pyrazolo[3,4-d]pyrimidin-4-one (2). White powder (61%): mp 220–222°C; IR (KBr, selected lines) cm⁻¹ 1688, 1644, 1595, 1569, 1384, 1309, 1168, 981, 773; ¹H NMR (DMSO-*d*₆) δ 3.90 (s, 3H, OCH₃), 4.80 (s, 2H, CH₂CO), 6.98–7.30 (m, 5H, aromatic), 7.60–7.68 (m, 2H, aromatic), 7.80–7.95 (m, 2H, aromatic), 8.23 (s, 1H, pyrazole), 12.90 (s, 1H, NH). Anal. (C₂₀H₁₆N₄O₃S) C, H, N, S.

2.1.4. 1,5-Dihydro-6-[[2-(3-methoxyphenyl)-2-oxoethyl]thio]-1-phenyl-4H-pyrazolo[3,4-d]pyrimidin-4-one (3). White powder (82%): mp 247–249°C dec; IR (KBr, selected lines) cm⁻¹ 1684, 1595, 1560, 1519, 1426, 1395, 1260, 1223, 1166; ¹H NMR (DMSO-*d*₆) δ 3.82 (s, 3H, OCH₃), 4.99 (s, 2H, CH₂CO), 6.90–7.02 (m, 2H, aromatic), 7.05–7.20 (m, 1H, aromatic), 7.25–7.40 (m, 1H, aromatic), 7.45–7.60 (m, 2H, aromatic), 7.65–7.81 (m, 3H, aromatic), 8.24 (s, 1H, pyrazole), 12.90 (s, 1H, NH). Anal. (C₂₀H₁₆N₄O₃S) C, H, N, S.

2.1.5. 1,5-Dihydro-6-[[2-(4-methoxyphenyl)-2-oxoethyl]thio]-1-phenyl-4H-pyrazolo[3,4-d]pyrimidin-4-one (4). White powder (44%): mp 252–254°C; IR (KBr, selected lines) cm⁻¹ 1686, 1600, 1572, 1512, 1423, 1398, 1311, 1294, 1174; ¹H NMR (DMSO-*d*₆) δ 3.91 (s, 3H, OCH₃), 4.93 (s, 2H, CH₂CO), 6.99–7.22 (m, 5H, aromatic), 7.68–7.90 (m, 2H, aromatic), 7.99–8.15 (m, 2H, aromatic), 8.22 (s, 1H, pyrazole), 12.87 (s, 1H, NH). Anal. (C₂₀H₁₆N₄O₃S) C, H, N, S.

2.1.6. 1,5-Dihydro-6-[[2-(4-methylphenyl)-2-oxoethyl]thio]-1-phenyl-4H-pyrazolo[3,4-d]pyrimidin-4-one (5). White powder (41%): mp 266–269°C; IR (KBr, selected lines) cm⁻¹ 3070, 1729, 1547, 1529, 1509, 1482, 1426, 1394, 764; ¹H NMR (DMSO-*d*₆) δ 2.46 (s, 3H, CH₃), 4.96 (s, 2H, CH₂CO), 6.90–7.10 (m, 2H, aromatic), 7.10–7.20 (m, 1H, aromatic), 7.38–7.50 (m, 2H, aromatic), 7.70–7.90 (m, 2H, aromatic), 7.90–8.10 (m, 2H, aromatic), 8.25 (s, 1H, pyrazole), 12.89 (s, 1H, NH). Anal. (C₂₀H₁₆N₄O₂S) C, H, N, S.

2.1.7. 1,5-Dihydro-6-[[2-(3-nitrophenyl)-2-oxoethyl]thio]-1-phenyl-4H-pyrazolo[3,4-d]pyrimidin-4-one (6). White powder (54%): mp 224–227°C; IR (KBr, selected lines) cm⁻¹ 1705, 1673, 1523, 1488, 1399, 1349, 1314, 1203, 1109; ¹H NMR (DMSO-*d*₆) δ 5.08 (s, 2H, CH₂CO), 6.90–7.15 (m, 3H, aromatic), 7.65–7.79 (m, 2H, aromatic), 7.85–8.10 (m, 1H, aromatic), 8.25 (m, 1H, pyrazole), 8.45–8.58 (m, 2H, aromatic), 8.65 (s, 1H, aromatic), 12.92 (s, 1H, NH). Anal. (C₁₉H₁₃N₅O₄S) C, H, N, S.

2.1.8. 1,5-Dihydro-6-[[2-(4-nitrophenyl)-2-oxoethyl]thio]-1-phenyl-4H-pyrazolo[3,4-d]pyrimidin-4-one (7). Yellow powder (53%): mp 250–251°C dec; IR (KBr, selected lines) cm⁻¹ 1709, 1673, 1567, 1526, 1493, 1397, 1346, 1223, 1194; ¹H NMR (DMSO-*d*₆) δ 5.04 (s, 2H, CH₂CO), 6.90–7.18 (m, 3H, aromatic), 7.65–7.75 (m, 2H, aromatic), 8.18–8.30 (m, 2H + 1H, aromatic + pyrazole), 8.30–8.40 (m, 2H, aromatic), 12.92 (s, 1H, NH). Anal. (C₁₉H₁₃N₅O₄S) C, H, N, S.

2.1.9. 6-[[2-(4-Chlorophenyl)-2-oxoethyl]thio]-1,5-dihydro-1-phenyl-4H-pyrazolo[3,4-d]pyrimidin-4-one (8). White powder (36%): mp 250–252°C; IR (KBr, selected lines) cm⁻¹ 1682, 1561, 1500, 1397, 1223, 1200, 1090, 984, 824; ¹H NMR (DMSO-*d*₆) δ 4.97 (s, 2H, CH₂CO), 6.90–7.10 (m, 2H, aromatic), 7.10–7.22 (m, 1H, aromatic), 7.58–7.90 (m, 4H, aromatic), 8.00–8.18 (m, 2H, aromatic), 8.23 (s, 1H, pyrazole), 12.90 (s, 1H, NH). Anal. (C₁₉H₁₃ClN₄O₂S) C, H, N, S.

2.1.10. 6-[[2-(4-Bromophenyl)-2-oxoethyl]thio]-1,5-dihydro-1-phenyl-4H-pyrazolo[3,4-d]pyrimidin-4-one (9). White powder (32%): mp 254–255°C; IR (KBr, selected lines) cm⁻¹ 1692, 1561, 1500, 1425, 1396, 1223, 1200, 984, 821; ¹H NMR (DMSO-*d*₆) δ 4.96 (s, 2H, CH₂CO), 6.95–7.10 (m, 2H, aromatic), 7.10–7.22 (m, 1H, aromatic), 7.70–7.90 (m, 4H, aromatic), 7.95–8.10 (m, 2H, aromatic), 8.23 (s, 1H, pyrazole), 12.90 (s, 1H, NH). Anal. (C₁₉H₁₃BrN₄O₂S) C, H, N, S.

2.1.11. 1,5-Dihydro-6-[[2-(4-fluorophenyl)-2-oxoethyl]thio]-1-phenyl-4H-pyrazolo[3,4-d]pyrimidin-4-one (10). White powder (71%): mp 247–250°C; IR (KBr, selected lines) cm⁻¹ 1702, 1686, 1596, 1564, 1500, 1392, 1220, 1155, 831; ¹H NMR (DMSO-*d*₆) δ 4.98 (s, 2H, CH₂CO), 6.95–7.10 (m, 2H, aromatic), 7.10–7.22 (m, 1H, aromatic), 7.39–7.60 (m, 2H, aromatic), 7.70–7.90 (m, 2H, aromatic), 8.10–8.20 (m, 2H, aromatic), 8.22 (s, 1H, pyrazole), 12.89 (s, 1H, NH). Anal. (C₁₉H₁₃FN₄O₂S) C, H, N, S.

2.1.12. General Procedure for the Synthesis of 6-Substituted Phenyl-1-phenyl-1H-pyrazolo[3,4-d]thiazolo[3,2-a]pyrimidin-4(1H)-one (11–13, 15, 16). A mixture of the suitable 1,5-dihydro-6-[[2-(substituted phenyl)-2-oxoethyl]thio]-1-phenyl-4H-pyrazolo[3,4-d]pyrimidin-4-one (**2–4**, **6**, and **7**) (2.46 mmol) and polyphosphoric acid (20 g) was stirred at 140°C for 2 h. After cooling, the mixture was poured into cold water, neutralized with a 10% sodium hydroxide solution. The solid obtained was collected, washed with water, dried,

and recrystallized from dimethylformamide. Using this procedure the following compounds were obtained.

2.1.13. 6-(2-Methoxyphenyl)-1-phenyl-pyrazolo[3,4-*d*]thiazolo[3,2-*a*]pyrimidin-4(1H)-one (**11**). White powder (53%): mp 247–249°C; IR (KBr, selected lines) cm^{-1} 1731, 1568, 1524, 1480, 1424, 1294, 1050, 1008, 778; ^1H NMR (DMSO- d_6) δ 3.78 (s, 3H, OCH₃), 6.98–7.45 (m, 5H + 1H, aromatic + thiazole), 7.50–7.65 (m, 2H, aromatic), 8.05–8.17 (m, 2H, aromatic), 8.35 (s, 1H, pyrazole). Anal. (C₂₀H₁₄N₄O₂S) C, H, N, S.

2.1.14. 6-(3-Methoxyphenyl)-1-phenyl-pyrazolo[3,4-*d*]thiazolo[3,2-*a*]pyrimidin-4(1H)-one (**12**). White powder (47%): mp 267–269°C; IR (KBr, selected lines) cm^{-1} 1724, 1587, 1546, 1521, 1480, 1399, 1242, 854, 753; ^1H NMR (DMSO- d_6) δ 3.68 (s, 3H, OCH₃), 6.96–7.19 (m, 2H, aromatic), 7.21 (s, 1H, thiazole), 7.32–7.52 (m, 3H, aromatic), 7.53–7.65 (m, 2H, aromatic), 8.02–8.12 (m, 2H, aromatic), 8.33 (s, 1H, pyrazole). Anal. (C₂₀H₁₄N₄O₂S) C, H, N, S.

2.1.15. 6-(4-Methoxyphenyl)-1-phenyl-pyrazolo[3,4-*d*]thiazolo[3,2-*a*]pyrimidin-4(1H)-one (**13**). White powder (60%): mp 278–280°C; IR (KBr, selected lines) cm^{-1} 3065, 1731, 1543, 1516, 1477, 1396, 1292, 1187, 764; ^1H NMR (DMSO- d_6) δ 3.82 (s, 3H, OCH₃), 6.90–7.00 (m, 2H, aromatic), 7.16 (s, 1H, thiazole), 7.38–7.45 (m, 3H, aromatic), 7.50–7.60 (m, 2H, aromatic), 8.05–8.15 (m, 2H, aromatic), 8.34 (s, 1H, pyrazole). Anal. (C₂₀H₁₄N₄O₂S) C, H, N, S.

2.1.16. 6-(3-Nitrophenyl)-1-phenyl-pyrazolo[3,4-*d*]thiazolo[3,2-*a*]pyrimidin-4(1H)-one (**15**). Yellow powder (61%): mp 254–256°C; IR (KBr, selected lines) cm^{-1} 1716, 1546, 1505, 1424, 1396, 1350, 1195, 1133, 787; ^1H NMR (DMSO- d_6) δ 7.35–7.48 (m, 1H + 1H, aromatic + thiazole), 7.55–7.75 (m, 3H, aromatic), 7.90–8.00 (m, 1H, aromatic), 8.05–8.12 (m, 2H, aromatic), 8.28–8.40 (m, 2H + 1H, aromatic + pyrazole). Anal. (C₁₉H₁₁N₅O₃S) C, H, N, S.

2.1.17. 6-(4-Nitrophenyl)-1-phenyl-pyrazolo[3,4-*d*]thiazolo[3,2-*a*]pyrimidin-4(1H)-one (**16**). Yellow powder (74%): mp > 330°C; IR (KBr, selected lines) cm^{-1} 1724, 1552, 1527, 1508, 1485, 1344, 1129, 764, 746; ^1H NMR (DMSO- d_6) δ 7.38–7.50 (m, 2H + 1H, aromatic + thiazole), 7.55–7.70 (m, 1H, aromatic), 7.70–7.82 (m, 2H, aromatic), 8.10–8.15 (m, 2H, aromatic), 8.20–8.30 (m, 2H, aromatic), 8.38 (s, 1H, pyrazole). Anal. (C₁₉H₁₁N₅O₃S) C, H, N, S.

2.1.18. General Procedure for the Synthesis of 6-Substituted Phenyl-1-phenyl-pyrazolo[3,4-*d*]thiazolo[3,2-*a*]pyrimidin-4(1H)-one (**14**, **17–19**). A mixture of the suitable 1,5-dihydro-6-[[2-(substituted phenyl)-2-oxoethyl]thio]-1-phenyl-4H-pyrazolo[3,4-*d*]pyrimidin-4-one (**5**, **8–10**) (1.86 mmol) and sulfuric acid (3.4 mL) was stirred at room temperature for 1 h. Then the solution was kept at room temperature for 4 days. After cooling, the mixture was poured into cold water and neutralized with a 10% solution of sodium hydroxide. The solid obtained was collected, washed with water, dried, and

recrystallized from dioxane, with the exception of compound **18** (recrystallization solvent: ethanol/dioxane). Using this procedure, the following compounds were obtained.

2.1.19. 6-(4-Methylphenyl)-1-phenyl-pyrazolo[3,4-*d*]thiazolo[3,2-*a*]pyrimidin-4(1H)-one (**14**). White powder (52%): mp 273–275°C; IR (KBr, selected lines) cm^{-1} 1728, 1546, 1508, 1482, 1425, 1392, 1187, 1129, 763; ^1H NMR (DMSO- d_6) δ 2.37 (s, 3H, CH₃), 7.18–7.25 (m, 2H + 1H, aromatic + thiazole), 7.28–7.45 (m, 3H, aromatic), 7.50–7.65 (m, 2H, aromatic), 8.02–8.15 (m, 2H, aromatic), 8.33 (s, 1H, pyrazole). Anal. (C₂₀H₁₄N₄OS) C, H, N, S.

2.1.20. 6-(4-Chlorophenyl)-1-phenyl-pyrazolo[3,4-*d*]thiazolo[3,2-*a*]pyrimidin-4(1H)-one (**17**). White powder (42%): mp 261–264°C; IR (KBr) cm^{-1} 1720, 1510, 1480, 1390, 1235, 1120, 1090, 990, 745; ^1H NMR (DMSO- d_6) δ 7.30 (s, 1H, thiazole), 7.38–7.50 (m, 7H, aromatic), 8.00–8.18 (m, 2H, aromatic), 8.35 (s, 1H, pyrazole). Anal. (C₁₉H₁₁ClN₄OS·(1/2)H₂O) C, H, N, S.

2.1.21. 6-(4-Bromophenyl)-1-phenyl-pyrazolo[3,4-*d*]thiazolo[3,2-*a*]pyrimidin-4(1H)-one (**18**). White powder (62%): mp 272–274°C; IR (KBr, selected lines) cm^{-1} 1706, 1576, 1546, 1482, 1395, 1190, 1066, 1003, 768; ^1H NMR (DMSO- d_6) δ 7.30 (s, 1H, thiazole), 7.40–7.52 (m, 3H, aromatic), 7.52–7.70 (m, 4H, aromatic), 8.05–8.15 (m, 2H, aromatic), 8.35 (s, 1H, pyrazole). Anal. (C₁₉H₁₁BrN₄OS) C, H, N, S.

2.1.22. 6-(4-Fluorophenyl)-1-phenyl-pyrazolo[3,4-*d*]thiazolo[3,2-*a*]pyrimidin-4(1H)-one (**19**). White powder (53%): mp 286–288°C; IR (KBr) cm^{-1} 1725, 1530, 1510, 1482, 1395, 1230, 820, 795, 740; ^1H NMR (DMSO- d_6) δ 7.15–7.35 (m, 2H + 1H, aromatic + thiazole), 7.35–7.95 (m, 5H, aromatic), 8.00–8.20 (m, 2H, aromatic), 8.34 (s, 1H, pyrazole). Anal. (C₁₉H₁₁FN₄OS) C, H, N, S.

2.2. Computational Methods

2.2.1. VS+. VS+ is an automatic procedure which allows converting information coded into the 3D GRID Molecular Interaction Fields into 128 physicochemically relevant descriptors [31]. The obtained descriptors concern molecular size and shape, hydrophilic and hydrophobic properties, hydrogen bonding, amphiphilic moments, and critical packing parameters. Pharmacokinetic descriptors related to solubility, metabolic stability, and cell permeability were also generated.

Surface properties such as shape, electrostatic forces, H-bonds, and hydrophobicity influenced the interaction of molecules with biological membranes. Therefore, potential polar and hydrophobic interaction sites around target molecules by the water (OH₂), the hydrophobic (DRY), and the carbonyl oxygen (O) and amide nitrogen (N1) probe [32] were characterized by the GRID force field.

The information contained in the Molecular Interaction Fields (MIF) is converted into a quantitative scale by calculating the volume or the surface of the interaction contours. The VS+ procedure is as follows:

- (i) First, the interactions of OH₂, DRY, O, and N1 probes around a target molecule generated the 3D molecular field.
- (ii) Then, the descriptors from the 3D maps, obtained in the first step, were calculated. These molecular descriptors, called VS+ descriptors, concern molecular size and shape, hydrophilic and hydrophobic regions and the balance between them, molecular diffusion, log P, log D, “charge state” descriptors, new 3D pharmacophoric descriptors, and descriptors of some appropriate ADME properties. The definition of all 128 VS+ descriptors was reported elsewhere [31].
- (iii) Finally, chemometric tools (PCA [33] and PLS [34]) are used to create relationships of the VS+ descriptor matrix with ADME properties.

The scheme of the VS+ programme steps and a detailed definition of VS+ descriptors have recently been reported [35].

The .mol2 files for 176 new molecules were generated and classified in 7 different classes based on their different chemical features for a better classification and identification: pyrrolopyrimidindione, pyrimidinketones, benzyloxyindole, indole, LCAPs, quinoline, and thiophene derivatives [15–25]. The structures of all compounds were reported in Supporting Information (SI).

The VS+ software was used to perform a Structure-Activity Relationship (QSAR) study using the default settings for protomers and conformers generations.

2.3. Biological Assays

2.3.1. Human Cell Lines (MCF-7 and MDA-MB-231). Two human breast adenocarcinoma cell lines, MCF-7 (ATCC number: HTB-22) and MDA-MB-231 (ATCC number: HTB26), have been cultured as previously reported [36]. MCF-7 cell line was maintained in D-MEM medium (Dulbecco's Modified Eagle Medium 1x; GIBCO, Cat number 31965-023 containing 1 g/L of D-glucose). MDA-MB-231 cell line was maintained in DMEM/F12 medium (Dulbecco's Modified Eagle Medium Ham's F12 Nutrient Mixture, 1x; GIBCO, Cat. number 21331-020), 1.5 mM L-glutamine, and MEM nonessential amino acid solution 1x (SIGMA M7145). Each medium was supplemented with 10% fetal ovine serum (FBS, Cat. number 10270-106, Life Technologies, Monza Italy) and 100 U/ml of penicillin-streptomycin (Cat. number 15140-122, Life Technologies, Monza Italy). The cell cultures were grown and incubated at 37°C in humidified atmosphere with 5% of CO₂ and 95% of air. The culture medium was changed twice a week.

2.3.2. Treatment with Antitumor Agents and MTT Colorimetric Assay. Human cancer cell line was plated in 96-well plates “Nunclon TM Microwell TM” (Nunc) and were incubated at 37°C. MTT assay was performed as reported by Barresi et al. [37]. After 24 h, cells were treated with the compounds (final concentration 0.01–100 μM). Untreated cells were used as controls. Microplates were incubated at 37°C in humidified atmosphere of 5% CO₂, 95% air for 3 days, and then cytotoxicity was measured with colorimetric assay based on the use of tetrazolium salt MTT (3-(4,5-dimethylthiazol-2-yl)-2,5-diphenyl tetrazolium bromide) [38]. The results were read on a multiwell scanning spectrophotometer (PlateReader AF2200, Eppendorf, Milan, Italy), using a wavelength of 570 nm. Each value was the average of six to eight wells (standard deviations were less than 15%). The GI₅₀ value was calculated according to NCI [39]: thus, GI₅₀ is the concentration of test compound where $100 \times (T - T_0) / (C - T_0) = 50$ (T is the optical density of the test well after a 72 h period of exposure to test drug; T_0 is the optical density at time zero; C is the control optical density). The cytotoxicity effect was calculated according to NCI when the optical density of treated cells was lower than the T_0 value using the following formula: $100 \times (T - T_0) / T_0 < 0$.

3. Results and Discussion

As a first approach we projected all the 176 compounds on the model previously published [12]. The PLS model after projection of the test set is shown in Figure 1: the predicted compounds are colored according to the different belonging classes: pyrrolopyrimidindione in green, pyrimidinketones in yellow, benzyloxyindole in light blue, indole in red, LCAPs in purple, quinoline in blu, and thiophene in white. The background of the PLS model is color-coded by the activity values against MCF-7 cell line, using a scale from red (active) to blue (inactive). The t_1 and t_2 values refer to the coordinates of each single compound within the plot.

Two outliers families, pyrrolopyrimidindione and thiophene derivatives, lying out of the confidence ellipse were discharged, probably due to some solubility and permeability problems.

Moreover, in order to increase the predictivity power, we performed the class model for each single subset discharging the correspondent outliers (SI). By using this strategy, we obtained a test set of 25 compounds that are the best representative molecules for each class (Figure 2).

Starting from the obtained test set, we decided to select 10 out of the 25 derivatives: 5 from active part of the graphic, red area, and 5 from the inactive one, blue area (Table 1). To validate our prediction we tested those compounds in vitro against MCF-7 and MDA-MB-231 cell lines using 5-fluorouracil (5-FU) as standard chemotherapy agent reference (Table 1). The biological characteristics of MCF7 and MDA-MB-231 are dissimilar: the first cell line is a representative model of ductal breast carcinoma, oestrogen receptor-positive, receptor tyrosine-protein kinase (erbB-2, HER2/neu) negative and responding to endocrine therapy,

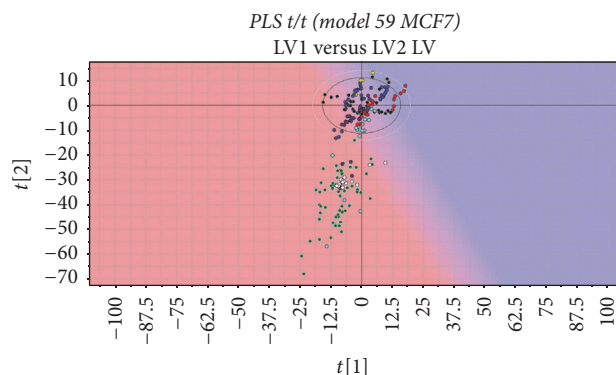


FIGURE 1: PLS t/t scores plot for the 176 selected compounds.

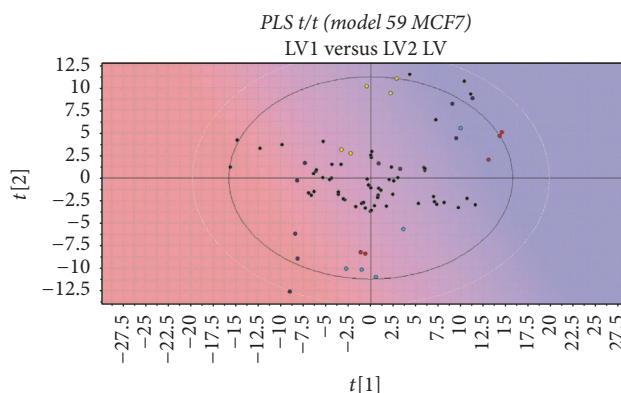


FIGURE 2: PLS t/t scores plot for 25 derivatives (yellow points) selected based on activity prediction: active, inactive, and moderately active.

while the MDA-MB-231 is oestrogen receptor-negative unresponsive to the same treatment.

The antiproliferative effects observed in Table 1 for compounds pyrimidinketone 2A, pyrimidinketone 2B, and quinoline 7B are stronger than same similar effect observed with the reference 5-FU in both cell lines. It is noteworthy that these compounds, with very low t_1 values in Figure 2, exhibit a very high activity, thus confirming the robustness of the PLS predictions from a quantitative point of view.

In Table 1, we report the experimental activity values, expressed as $\log GI_{50}$, for the 10 tested compounds and VS+ predicted values. In particular, in red we report the 5 compounds predicted active (Table 1), while in blue we report the remaining 5 predicted inactive. In silico predictions were confirmed for most of the compounds tested in vitro. Two marked compounds in the table, predicted active, resulted inactive in the experimental test. However, it should be noted that these two compounds showed some solubility problem during the in vitro procedure, even if we added 1% of DMSO; they gave flocculation; thus data relative to these compounds are not reliable.

4. Conclusion

The predictivity power of the model previously published from our group was confirmed using different type of heterocyclic compounds. Three of these derivatives showed good antiproliferative in vitro activity against MCF-7 and MDA-MB-231 cell lines. The MDA-MB-231 cell line represents a triple-negative breast cancer without oestrogen receptor (ER), progesterone receptor (PR), and epidermal growth factor receptor 2 (HER2), associated with strong aggressiveness, poor prognosis, and unresponsiveness to the usual endocrine therapies. The antiproliferative effects observed on MCF-7 and MDA-MB-231 are worthy of attention to develop molecules that are able to attack the breast tumor oestrogen receptor-positive and/or oestrogen receptor-negative. Studies aimed at the elucidation of the above mechanism pathways are in progress.

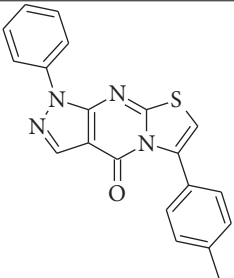
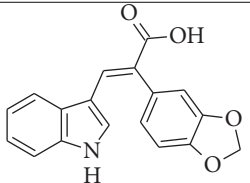
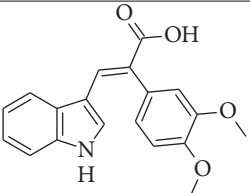
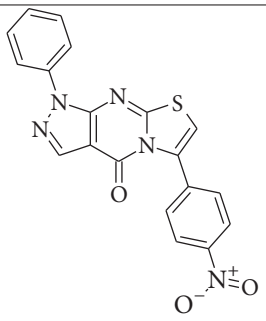
Conflicts of Interest

The authors declare no conflicts of interest regarding the publication of this paper.

TABLE 1: Molecular structures, in vitro activity on MCF-7 and MDA-MB-231 cell lines, and in silico activity values for the ten selected compounds and 5-FU. Activity values expressed as $\log GI_{50}$.

Molecule name	Molecular structure	MCF7 experimental activity $\log GI_{50}/\mu M \pm SD^*$	MDA-MB-231 experimental activity $\log GI_{50}/\mu M \pm SD^*$	Predicted activity versus MCF7
Pyrimidinketone 2A		-5.20 ± 0.7	-4.8 ± 0.4	-6.08
Quinoline 7B		-4.80 ± 0.6	-4.3 ± 0.5	-6.72
Pyrimidinketone 2B		-4.90 ± 0.8	-4.6 ± 0.3	-6.21
X LCAPs 8A		>-4.00		-6.86
X Quinoline 7A		>-4.00	-4.8	-6.83
Indole 2B		>-4.00	-4.6 ± 0.6	-3.83

TABLE I: Continued.

Molecule name	Molecular structure	MCF7 experimental activity $\log GI_{50}/\mu M \pm SD^*$	MDA-MB-231 experimental activity $\log GI_{50}/\mu M \pm SD^*$	Predicted activity versus MCF7
Pyrimidinketone 3B		>-4.00	NA	-4.00
Indole 3E		>-4.00	>-4.00	-3.70
Indole 3D		>-4.00	>-4.00	-4.00
Pyrimidinketone 2D		>-4.00	>-4.00	-4.00
5-FU		-5.40 ± 0.7	-5.1 ± 0.4	—

*Each value represents the mean \pm SD of six to eight wells. NA, not available.

Acknowledgments

The authors thank University of Catania for financial support.

References

- [1] R. L. Siegel, K. D. Miller, and A. Jemal, "Cancer statistics, 2015," *CA Cancer Journal for Clinicians*, vol. 65, no. 1, pp. 5–29, 2015.
- [2] V. Diaby, R. Tawk, V. Sanogo, H. Xiao, and A. J. Montero, "A review of systematic reviews of the cost-effectiveness of hormone therapy, chemotherapy, and targeted therapy for breast cancer," *Breast Cancer Research and Treatment*, vol. 151, no. 1, pp. 27–40, 2015.
- [3] A. Toss and M. Cristofanilli, "Molecular characterization and targeted therapeutic approaches in breast cancer," *Breast Cancer Research*, vol. 17, no. 1, article 60, 2015.
- [4] L. Dossus, M.-C. Boutron-Ruault, R. Kaaks et al., "Active and passive cigarette smoking and breast cancer risk: results from the EPIC cohort," *International Journal of Cancer*, vol. 134, no. 8, pp. 1871–1888, 2014.
- [5] D. P. McDonnell, S. Park, M. T. Goulet et al., "Obesity, cholesterol metabolism, and breast cancer pathogenesis," *Cancer Research*, vol. 74, no. 18, pp. 4976–4982, 2014.
- [6] V. Rosato, C. Bosetti, E. Negri et al., "Reproductive and hormonal factors, family history, and breast cancer according to the hormonal receptor status," *European Journal of Cancer Prevention*, vol. 23, no. 5, pp. 412–417, 2014.
- [7] T. K. Choueiri, E. L. Mayer, Y. Je et al., "Congestive heart failure risk in patients with breast cancer treated with bevacizumab," *Journal of Clinical Oncology*, vol. 29, no. 6, pp. 632–638, 2011.
- [8] S. L. Schreiber, "Organic synthesis toward small-molecule probes and drugs," *Proceedings of the National Academy of Sciences*, vol. 108, no. 12, pp. 4881–4886, 2011.

- Sciences of the United States of America*, vol. 108, no. 17, pp. 6699–6702, 2011.
- [9] T. T. Ashburn and K. B. Thor, “Drug repositioning: identifying and developing new uses for existing drugs,” *Nature Reviews Drug Discovery*, vol. 3, no. 8, pp. 673–683, 2004.
- [10] M. E. Welsch, S. A. Snyder, and B. R. Stockwell, “Privileged scaffolds for library design and drug discovery,” *Current Opinion in Chemical Biology*, vol. 14, no. 3, pp. 347–361, 2010.
- [11] A. Gomtsyan, “Heterocycles in drugs and drug discovery,” *Chemistry of Heterocyclic Compounds*, vol. 48, no. 1, pp. 7–10, 2012.
- [12] V. Barresi, C. Bonaccorso, G. Consiglio et al., “Modeling, design and synthesis of new heteroaryl ethylenes active against the MCF-7 breast cancer cell-line,” *Molecular BioSystems*, vol. 9, no. 10, pp. 2426–2429, 2013.
- [13] V. La Pietra, G. La Regina, A. Coluccia et al., “Design, synthesis, and biological evaluation of 1-phenylpyrazolo[3,4-e]pyrrolo[3,4-g]indolizine-4,6(1H,5H)-diones as new glycogen synthase kinase-3 β inhibitors,” *Journal of Medicinal Chemistry*, vol. 56, no. 24, pp. 10066–10078, 2013.
- [14] M. G. Perrone, P. Vitale, A. Panella, C. G. Fortuna, and A. Scilimati, “General role of the amino and methylsulfamoyl groups in selective cyclooxygenase(COX)-1 inhibition by 1,4-diaryl-1,2,3-triazoles and validation of a predictive pharmacometric PLS model,” *European Journal of Medicinal Chemistry*, vol. 94, pp. 252–264, 2015.
- [15] G. Forte, C. G. Fortuna, L. Salerno et al., “Antitumor properties of substituted (α E)- α -(1H-indol-3-ylmethylene)benzeneacetic acids or amides,” *Bioorganic and Medicinal Chemistry*, vol. 21, no. 17, pp. 5233–5245, 2013.
- [16] E. Patanè, V. Pittalà, F. Guerrero et al., “Synthesis of 3-arylpiperazinylalkylpyrrolo[3,2-d]pyrimidine-2,4-dione derivatives as novel, potent, and selective α 1-adrenoceptor ligands,” *Journal of Medicinal Chemistry*, vol. 48, no. 7, pp. 2420–2431, 2005.
- [17] V. Pittalà, M. Modica, G. Romeo et al., “A facile synthesis of new 2-carboxamido-3-carboxythiophene and 4,5,6,7-tetrahydro-2-carboxamido-3-carboxythieno[2,3-c]pyridine derivatives as potential endothelin receptors ligands,” *Farmaco*, vol. 60, no. 9, pp. 711–720, 2005.
- [18] V. Pittalà, M. Modica, L. Salerno et al., “Synthesis and endothelin receptor binding affinity of a novel class of 2-substituted-4-aryl-3-quinolinecarboxylic acid derivatives,” *Medicinal Chemistry*, vol. 4, no. 2, pp. 129–137, 2008.
- [19] V. Pittalà, G. Romeo, L. Materia et al., “Novel (E)- α -[(1H-indol-3-yl)methylene]benzeneacetic acids as endothelin receptor ligands,” *Farmaco*, vol. 60, no. 9, pp. 731–738, 2005.
- [20] V. Pittalà, G. Romeo, L. Salerno et al., “3-Arylpiperazinylethyl-1H-pyrrolo[2,3-d]pyrimidine-2,4(3H,7H)-dione derivatives as novel, high-affinity and selective α 1-adrenoceptor ligands,” *Bioorganic and Medicinal Chemistry Letters*, vol. 16, no. 1, pp. 150–153, 2006.
- [21] V. Pittalà, M. A. Siracusa, M. N. Modica et al., “Synthesis and molecular modeling of 1H-pyrrolopyrimidine-2,4-dione derivatives as ligands for the α 1-adrenoceptors,” *Bioorganic and Medicinal Chemistry*, vol. 19, no. 17, pp. 5260–5276, 2011.
- [22] M. A. Siracusa, L. Salerno, M. N. Modica et al., “Synthesis of new arylpiperazinylalkylthiobenzimidazole, benzothiazole, or benzoxazole derivatives as potent and selective 5-HT_{1A} serotonin receptor ligands,” *Journal of Medicinal Chemistry*, vol. 51, no. 15, pp. 4529–4538, 2008.
- [23] G. Romeo, L. Materia, M. N. Modica et al., “Novel 4-phenylpiperidine-2,6-dione derivatives. Ligands for α 1-adrenoceptor subtypes,” *European Journal of Medicinal Chemistry*, vol. 46, no. 7, pp. 2676–2690, 2011.
- [24] L. Salerno, V. Pittalà, M. N. Modica et al., “Structure-activity relationships and molecular modeling studies of novel arylpiperazinylalkyl 2-benzoxazolones and 2-benzothiazolones as 5-HT₇ and 5-HT_{1A} receptor ligands,” *European Journal of Medicinal Chemistry*, vol. 85, pp. 716–726, 2014.
- [25] L. Salerno, M. Siracusa, F. Guerrero et al., “Synthesis of new 5-phenyl[1,2,4]triazole derivatives as ligands for the 5-HT_{1A} serotonin receptor,” *Arxiv*, vol. 2004, no. 5, pp. 312–324, 2004.
- [26] F. M. Awadallah, G. A. Piazza, B. D. Gary, A. B. Keeton, and J. C. Canzoneri, “Synthesis of some dihydropyrimidine-based compounds bearing pyrazoline moiety and evaluation of their antiproliferative activity,” *European Journal of Medicinal Chemistry*, vol. 70, pp. 273–279, 2013.
- [27] V. Pittalà and D. Pittalà, “Latest advances towards the discovery of 5-HT₇ receptor ligands,” *Mini-Reviews in Medicinal Chemistry*, vol. 11, no. 13, pp. 1108–1121, 2011.
- [28] M. M. Ghorab, M. G. El-Gazzar, and M. S. Alsaïd, “Design and synthesis of novel thiophenes bearing biologically active aniline, aminopyridine, benzylamine, nicotinamide, pyrimidine and triazolopyrimidine moieties searching for cytotoxic agents,” *Acta Polonicae Pharmaceutica*, vol. 71, no. 3, pp. 401–407, 2014.
- [29] B. E. Evans, K. E. Rittle, M. G. Bock et al., “Methods for drug discovery: development of potent, selective, orally effective cholecystokinin antagonists,” *Journal of Medicinal Chemistry*, vol. 31, no. 12, pp. 2235–2246, 1988.
- [30] S. Guccione, M. Modica, J. Longmore et al., “Synthesis and NK-2 antagonist effect of 1,6-diphenyl-pyrazolo [3,4-d]-thiazolo[3,2-a]4H-pyrimidin-4-one,” *Bioorganic and Medicinal Chemistry Letters*, vol. 6, no. 1, pp. 59–64, 1996.
- [31] G. Cruciani, P. Crivori, P.-A. Carrupt, and B. Testa, “Molecular fields in quantitative structure-permeation relationships: the VolSurf approach,” *Journal of Molecular Structure: THEOCHEM*, vol. 503, no. 1-2, pp. 17–30, 2000.
- [32] E. Carosati, S. Sciabola, and G. Cruciani, “Hydrogen bonding interactions of covalently bonded fluorine atoms: from crystallographic data to a new angular function in the GRID force field,” *Journal of Medicinal Chemistry*, vol. 47, no. 21, pp. 5114–5125, 2004.
- [33] S. Wold and M. Sjöström, “SIMCA: a method for analyzing chemical data in terms of similarity and analogy,” in *Chemometrics: Theory and Application*, vol. 52 of ACS Symposium Series, pp. 243–282, American Chemical Society, Washington, DC, USA, 1977.
- [34] S. Wold, C. Albano, W. J. Dunn et al., “Multivariate data analysis in chemistry,” in *Chemometrics*, vol. 138 of NATO ASI Series, pp. 17–95, Springer, Dordrecht, The Netherlands, 1984.
- [35] C. G. Fortuna, V. Barresi, G. Berellini, and G. Musumarra, “Design and synthesis of trans 2-(furan-2-yl)vinyl heteroaromatic iodides with antitumor activity,” *Bioorganic and Medicinal Chemistry*, vol. 16, no. 7, pp. 4150–4159, 2008.
- [36] A. Accardo, L. Del Zoppo, G. Morelli et al., “Liposome antibody-ionophore conjugate antiproliferative activity increases by cellular metallostasis alteration,” *MedChemComm*, vol. 7, no. 12, pp. 2364–2367, 2016.
- [37] V. Barresi, A. Trovato-Salinaro, G. Spampinato et al., “Transcriptome analysis of copper homeostasis genes reveals coordinated upregulation of SLC31A1, SCO1, and COX11 in colorectal cancer,” *FEBS Open Bio*, vol. 6, no. 8, pp. 794–806, 2016.

- [38] T. Mosmann, "Rapid colorimetric assay for cellular growth and survival: application to proliferation and cytotoxicity assays," *Journal of Immunological Methods*, vol. 65, no. 1-2, pp. 55-63, 1983.
- [39] U. Scherf, D. T. Ross, M. Waltham et al., "A gene expression database for the molecular pharmacology of cancer," *Nature Genetics*, vol. 24, no. 3, pp. 236-244, 2000.

